DOI https: //doi. org/10.1007/s11595-022-2652-6

The Combined Impact of Magnetic Field and Chloride Ion Concentration on Corrosion Behavior of Al-Mg Alloys

ZHANG Xin[1*], HUANG Lianpeng[1], TAO Jiahao[1], WANG Zehua[1], ZHOU Zehua[1], CAI Xin[1], WEN Tao[2]

(1. College of Mechanics and Materials, Hohai University, Nanjing 210098, China; 2. Beijing Yubing Water Hydraulic Survey Planning Design Co. Ltd. Jiangsu Branch, Nanjing 211111, China)

Abstract: The impact of magnetic field on the corrosion behavior of Al-Mg-xR$_E$/Fe alloys in NaCl solutions with concentrations of 1.5wt%, 3.5wt%, and 5.5wt% were studied by microstructure observation, immersion test, and electrochemical test. The combined impacts of magnetic field and chloride ion concentration on the corrosion behavior of Al-Mg alloys with various electrode potential phases were discussed. The results indicate that Al-3.0Mg-xR$_E$/Fe alloys corrode faster and have a higher pitting corrosion potential in the NaCl solution with a higher concentration. In addition, a magnetic field can lower the pitting sensitivity and corrosion rate of Al-3.0Mg and Al-3.0Mg-0.2R$_E$/Fe alloys in NaCl solution with different concentrations. However, at a higher concentration of NaCl solution, the magnetic field has a weaker inhibiting effect on corrosion rate and pitting sensitivity. In NaCl solutions with concentrations of 1.5wt% and 3.5wt%, the corrosion rate and pitting sensitivity of Al-3.0Mg-1.0R$_E$/Fe alloys can be reduced by a magnetic field. However, in NaCl solution with the concentration of 5.5wt%, the corrosion rate of the alloys is increased by a magnetic field.

Key words: magnetic field; corrosion behavior; chloride ion concentration; different electrode potential phases

1 Introduction

For the development of electronic and communication technology, many communication facilities have been built followed by the emergence of complex magnetic fields. Because of their excellent corrosion resistance, high strength, and ductility, Al-Mg alloys are intensively used in marine engineering materials[1-4]. However, pitting corrosion usually happens in aluminum alloys, causing the failure of the equipment and safety hazards[5-10]. In the presence of a magnetic field, the corrosion performance of Al-Mg alloy will be more complicated in high concentration chloride anion solution.

The impact of magnetic fields on the corruption behavior of metals has been studied by many researchers[11-27]. When metals are corroded, the moving charged particles are subject to additional forced induced by the presence of magnetic field, such as paramagnetic gradient force, Lorentz force, and gradient magnetic force[11,12]. Magnetic field have different effects on the corrosion behavior of various metals. When there are no paramagnetic ions in the corrosion system, such as copper and zinc alloys, the paramagnetic gradient force barely has almost no effect on the mass transport. The magnetic field usually accelerates the movement of ions in the corrosion process, resulting in the increasing corrosion rate of metals[13-18]. However, when paramagnetic ions are present or produced in the corrosion process of metals including iron and aluminum alloys, the paramagnetic ions are subject to the paramagnetic gradient force, leading to a gradient in the concentration of the paramagnetic ions, which will have complicated effects on corrosion behavior[19-25].

The impact of a magnetic field on the corrosion behavior of metals changes with different solutions. In NaCl solution, the corrosion rate of copper can be accelerated by the presence of magnetic field, while in the HNO_3 solution, the corrosion rate is reduced by the magnetic field[14,15]. When the magnetic field is withdrawn from acidic solutions, the OCP of iron experiences a negative shift. In contrast, when the magnetic field is withdrawn from neutral solutions, the OCP does not have significant change[24]. In the corrosion process, the second phases in the metal usually work as an an-

---

(Received: Sept. 12, 2021; Accepted: Jan. 10, 2022)

*Corresponding author: ZHANG Xin(张欣): Assoc. Prof.; Ph D; E-mail: zhangxin.007@163.com

Funded by the National Natural Science Foundation of China (No. 51909071), the Natural Science Foundation of Jiangsu Province (No. BK20190493), and the Fundamental Research Funds for the Central Universities (No. B220202040)

ode or cathode to aggravate the corrosion of the metal in nearby areas. We do not yet have a clear understanding of the effect of the magnetic field on the corruption behavior of the metal with various potential phases. Therefore, the combined impact of magnetic field and corrosion solution on the corruption performance of the metals containing various electrode potential phases is very complex.

In this study, the impact of magnetic field on the corrosion behavior of Al-Mg-xR$_E$/Fe alloys in NaCl solutions with concentrations of 1.5wt%, 3.5wt%, and 5.5wt% was discussed. In addition, the combined impact of magnetic field and chloride ion concentration on Al-Mg alloy's corrosion performance with various electrode potential phases were analyzed.

2 Experimental

An electrical resistance furnace was used to melt pure Al (99.7wt%) and Mg (99.9wt%) ingots at 720 ℃ in a graphite crucible. In order to obtain the Al-3.0Mg, Al-3.0Mg-0.2R$_E$/Fe and Al-3.0Mg-1.0R$_E$/Fe alloys for the immersion test and electrochemical test, the R6535 mischmetal (61.5wt% Ce and 37.3wt% La) or AlFe10 master alloy was pressed into the molten aluminum.

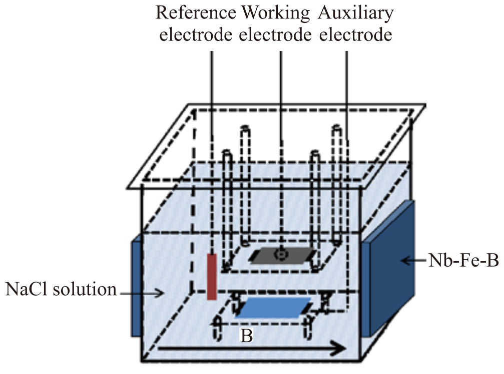

Fig.1 Device for electrochemical test

The immersion test was conducted in NaCl solution with the concentration of 1.5wt%, 3.5wt%, and 5.5wt% in the absence of magnetic field and under a magnetic field with the strength of 0.4 T for 7 days. The magnetic field was produced by an Nd-Fe-B permanent magnet. After the immersion test, the corrosion morphology of the samples was obtained by Hitachi S-3400 N scanning electron microscopy (SEM) and the chemical composition of the metals was analyzed by Horiba EX250 energy dispersive spectroscopy (EDS).

The samples for the electrochemical test were covered with a layer of epoxy resin, and a remaining surface area of about 1 cm^2 was exposed to the NaCl solution. Before the test, 2000 SiC papers were used to polish the surface of the samples to a mirror finish. We conducted the electrochemical test in the NaCl solutions with concentrations of 1.5wt%, 3.5wt%, and 5.5wt% in the absence of a magnetic field and under a 0.4 T magnetic field. The experiment was conducted with the PARSTAT 2273 electrochemical system containing three electrodes, *i e*, a working electrode (specimen electrode), a reference electrode (saturated calomel electrode), and a counter electrode (platinum wire), as shown in Fig.1. When the OCP became stable, the potentiodynamic polarization test was conducted at a scanning rate of 1 mV/s. All the tests were repeated three times or more to ensure the accuracy of the results. The cathode extrapolation was used to plot the Tafel curves because in the anode branch, there existed a passive region with the fixed current; while in the anode polarization, there was no Tafel region.

3 Results and discussion

Fig.2 shows corroded surface morphology of Al-3.0Mg alloys with various addition of R$_E$ or Fe after 7 days immersion test in NaCl solutions with the concentration of 1.5wt%, 3.5wt%, and 5.5wt%. Some skeletal second phases exist in the alloys. Based on previous studies[28,29], the skeletal phase in Al-3.0Mg alloy is the FeAl$_3$ phase. The addition of rare earth into the alloys cause a decrease in the amount of skeletal FeAl$_3$ phases and an increase in the amount of skeletal Al$_4$Ce/Al$_4$La phases. On the other hand, the addition of Fe to the samples result in a large amount and size of FeAl$_3$ phases. The more the added Fe, the more significant the increase.

There are some pitting holes on the corroded surface of Al-3.0Mg-xR$_E$/Fe alloys. With the increase of the concentration of NaCl, the amount and dimension of pitting holes increase significantly. It means that a high concentration of NaCl solution can promote the generation and growth of pitting corrosion in Al-Mg alloys. When more R$_E$ is added, the amount and dimension of pitting holes show a trend of first increasing and then decreasing. The fewest and smallest pitting holes are observed on the surface of Al-3.0Mg-0.2R$_E$ alloy, while the most and biggest pitting holes are observed on the surface of Al-3.0Mg-1.0R$_E$ alloy. Adding 0.2% R$_E$ inhibit the generation and growth of pitting holes, while adding 1.0% R$_E$ promote this process. With the increase of Fe addition, the amount and dimension of pitting holes increase steadily. It means that the addition of Fe led to the promotion of the generation and growth of pitting corrosion.

Fig.3 shows the morphologies of pitting holes on Al-3.0Mg-1.0R$_E$ and Al-3.0Mg-1.0Fe alloys after immersion test in the NaCl solution with the concentration of 5.5wt% for 7 days. The product from the cor-

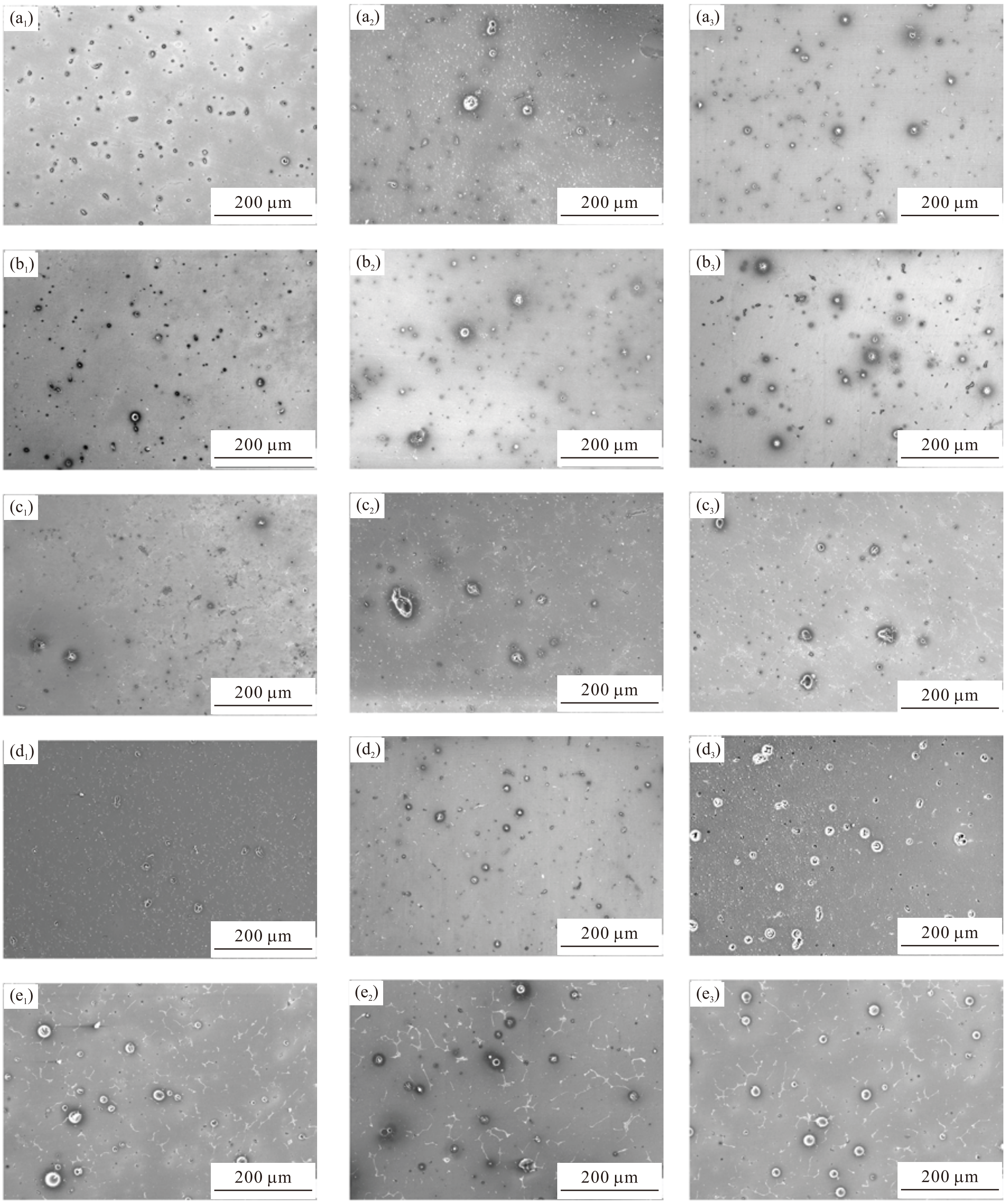

Fig.2 Surface morphology of Al-3.0 Mg with various addition of R_E or Fe in NaCl solutions with the concentrations of 1.5wt% (1), 3.5wt% (2) and 5.5wt% (3) for 7 days: (a) 0% R_E or Fe; (b) 0.2% R_E; (c) 1.0% R_E; (d) 0.2% Fe; (e) 1.0% Fe

rosion process was analyzed by EDS. The results are shown in Table 1. The pitting area of Al-3.0Mg-1.0R_E alloy contains 42.81wt% Al, 1.34wt% Mg, 38.22wt% O, 12.49wt% Ce, and 5.15wt% La. The result reveals the development of pitting corrosion in or around the region of Al_4Ce/Al_4La phases. The pitting area of Al-3.0Mg-1.0Fe alloy contains 34.85wt% Al, 1.92wt% Mg, 31.34wt% O, and 31.89wt% Fe, which reveals the development of pitting corrosion in or around the region of the $FeAl_3$ phase. The second phases have different electrode potentials, so they experience different types of corrosion. Compared with aluminum, the electrode potential of Al_4Ce/Al_4La phases is lower, and it acts as an anode to protect the Al substrate. However, self-corrosion of the Al_4Ce/Al_4La phase occurs readily, thus damaging the oxide film[30]. Consequently, the pitting corrosion holes are developed with the appearance of holes. These pitting holes are shown in Fig.3(a). On the contrary, the electrode potential of $FeAl_3$ phases (−0.56 V) is higher than that of aluminum (−0.85 V). Therefore, $FeAl_3$ phases work as a cathode, which can worsen the corrosion of the Al substrate. Consequently,

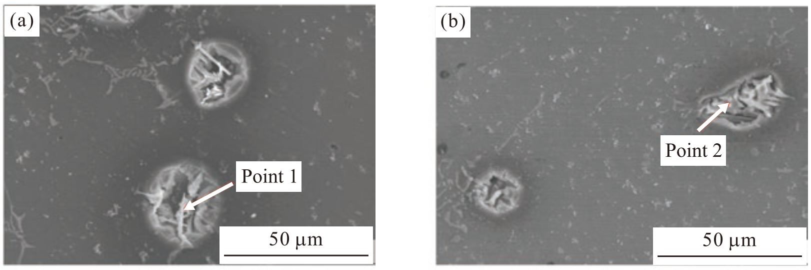

Fig.3 Surface morphology of Al-3.0Mg-1.0R$_E$/Fe alloy after immersion in NaCl solution with the concentration of 5.5wt% for 7 days: (a) Al-3.0Mg-1.0R$_E$ alloy; (b) Al-3.0Mg-1.0Fe alloy

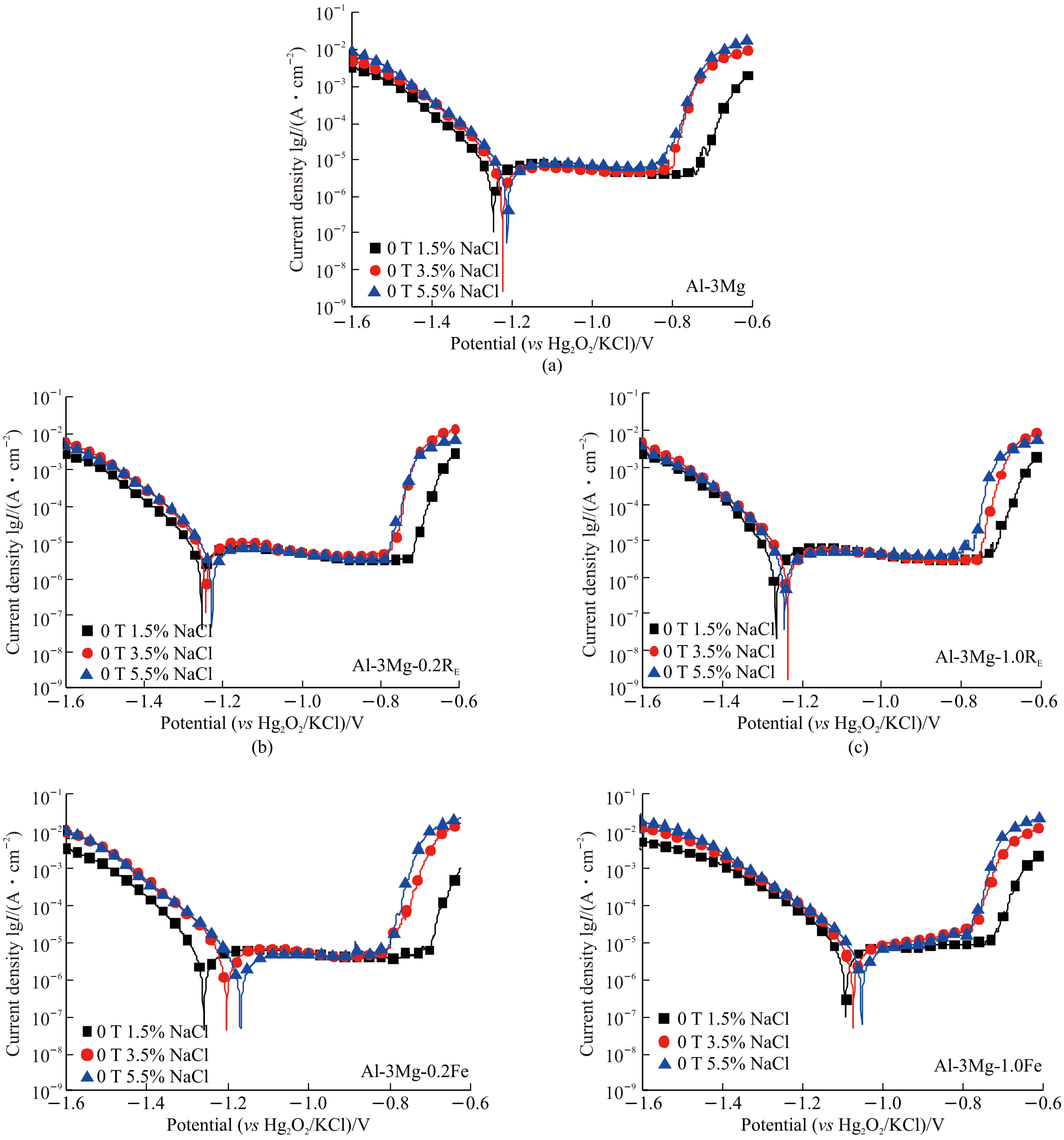

(a)

(b)

(c)

(d)

(e)

Fig.4 Potentiodynamic polarization curves of Al-3.0 Mg alloys containing various contents of R$_E$/Fe in 1.5wt%/3.5wt%/5.5wt% NaCl solution: (a) 0% R$_E$ or Fe; (b) 0.2% R$_E$; (c) 1.0% R$_E$; (d) 0.2% Fe; (e) 1.0% Fe

the pitting corrosion holes have island-like distribution, which are shown in Fig.3(b). During the corrosion process, the generation and damage of passivation film are cyclical. In general, pitting corrosion is developed nearby the second phase and start to develop when the passivation film in that area cracked. Therefore, the contents and dimension of the second phase are the determining factors for the number and dimension of the pitting holes. Specifically, when there are a larger number of second phases with bigger sizes, there are more pitting holes and their size is larger, and the corrosion is severer.

Table 1 EDS analysis on Al-3.0Mg-1.0R$_E$/Fe alloy after immersion in NaCl solution with the concentration of 5.5wt% for 7 days/wt%

	Al	Mg	O	Fe	Ce	La
Point 1	42.81	1.34	38.22	/	12.49	5.15
Point 2	34.85	1.92	31.34	31.89	/	/

Table 2 Values of E_{corr}, i_{corr}, and E_{pit} of Al-3.0Mg alloys containing various contents of R$_E$/Fe in 1.5wt%/3.5wt%/5.5wt% NaCl solution derived from the polarization curves

		E_{corr}/ V	i_{corr}/(μA·cm^{-2})	E_{pit}/V
Al-3.0Mg	1.5% NaCl	−1.248	4.474	−0.777
	3.5% NaCl	−1.216	7.253	−0.821
	5.5% NaCl	−1.211	8.263	-0.837
Al-3.0Mg-0.2R$_E$	1.5% NaCl	−1.256	3.566	−0.740
	3.5% NaCl	−1.243	6.788	−0.793
	5.5% NaCl	−1.232	8.518	−0.808
Al-3.0Mg-1.0R$_E$	1.5% NaCl	−1.269	4.721	−0.765
	3.5% NaCl	−1.261	9.130	−0.836
	5.5% NaCl	−1.248	9.873	−0.841
Al-3.0Mg-0.2Fe	1.5% NaCl	−1.261	6.070	−0.773
	3.5% NaCl	−1.240	10.301	−0.841
	5.5% NaCl	−1.173	10.991	−0.851
Al-3.0Mg-1.0Fe	1.5% NaCl	−1.099	7.331	−0.749
	3.5% NaCl	−1.073	8.408	−0.805
	5.5% NaCl	−1.019	12.661	−0.811

The potentiodynamic polarization curves of Al-3.0Mg-xR$_E$/Fe alloys are shown in Fig.4. The corrosion potential E_{corr}, corrosion current density i_{corr}, and pitting corrosion potential E_{pit} of the alloys are listed in Table 2. With the increase of NaCl concentration, the values of E_{corr} and i_{corr} of all alloys increase, while the value of E_{pit} decrease. It means that the corrosion rate and pitting corrosion potential of Al-3.0Mg-xR$_E$/Fe alloys are higher in NaCl solutions with a higher concentration. As the R_E addition increase, the values of E_{corr} and E_{pit} show a trend of first increasing and then decreasing, while the value of i_{corr} show the trend of first decreasing and then increasing. Adding 0.2wt% R_E can improve the purification of the aluminum molten and decrease the amount of FeAl$_3$ phases, thereby enhancing the corrosion resistance of Al-3.0Mg alloys. However, when the added amount of R_E is excessive, the amount of Al$_4$Ce/Al$_4$La phases increase, and then the corrosion resistance of the alloys is reduced[30]. As the iron content become higher, the shifting direction of E_{corr} and E_{pit} values is first to the negative direction, and then to the positive direction, while i_{corr} value have a steady increase. The E_{corr} and E_{pit} values of Al-3.0Mg-0.2Fe alloy are the smallest, and the i_{corr} values of Al-3.0Mg-1.0Fe alloy are the biggest. The results indicate that when 0.2wt% Fe is added, the corrosion and pitting sensitivity of Al-3.0 Mg alloy are increased. At the same time, adding 1.0wt% Fe led to an increasing in the corrosion rate of the alloys. When 1.0wt% Fe is added, the corrosive behavior and characteristics of Al-3.0 Mg alloy are changed. The potentiodynamic polarization curves of Al-3.0Mg-1.0Fe alloy have a less pronounced passivation region, indicating that the corrosion characteristic of the alloys changed from pitting corrosion to uniform corrosion.

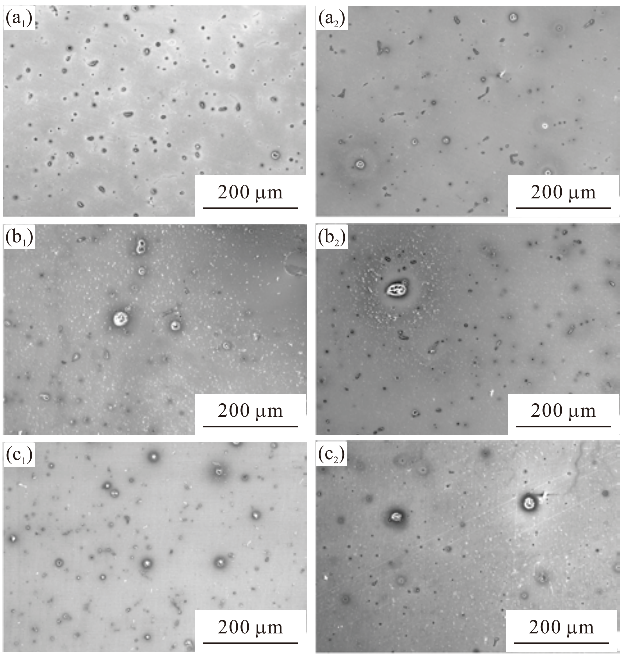

Fig.5 Surface morphologies of corroded Al-3.0Mg alloy in NaCl solution in the absence of magnetic field and under a magnetic field with the strength of 0.4 T: (a$_1$) 1.5% NaCl, 0 T; (a$_2$) 1.5% NaCl, 0.4 T; (b$_1$) 3.5% NaCl, 0 T; (b$_2$) 3.5% NaCl, 0.4 T; (c$_1$) 5.5% NaCl, 0 T; (c$_2$) 5.5% NaCl, 0.4 T

Fig.5 shows the corrosion surface of Al-3.0Mg alloys after immersion in NaCl solution with the concentrations of 1.5wt%, 3.5wt%, and 5.5wt% in the absence of a magnetic field and under a magnetic field of 0.4 T. At magnetic field with the strength of 0.4 T, the pitting holes of Al-3.0Mg alloys are smaller and fewer than those in the absence of a magnetic field, which indicates that, in the corrosion process of Al-3.0Mg alloy, the presence of a magnetic field can prevent the pitting holes from forming and growing.

In the presence and absence of a magnetic field of the strength of 0.4 T, the potentiodynamic polarization curves of Al-3.0Mg alloy are plotted in Fig.6. The values of E_{corr}, i_{corr}, and E_{pit} of the alloys are summarized in Table 3. The presence of a magnetic field led to the positive shift of E_{corr} and E_{pit}. At the same time, the values of i_{corr} of Al-3.0Mg alloy under 0.4 T magnetic field are lower than the values in the absence of magnetic field. This result reveals that the presence of the magnetic field can decrease the corrosion and pitting corrosion sensibility and corrosion rate of Al-3.0Mg alloys in NaCl solutions with the concentrations of 1.5wt%, 3.5wt%, and 5.5wt%.

With the increase of NaCl concentration, the values of $i_{\mathrm{corr(0.4T)}}-i_{\mathrm{corr(0T)}}$ of Al-3.0Mg alloys increase from -1.350 to -0.310 μA·cm^{-2}, while the values of $E_{\mathrm{pit(0.4T)}}-E_{\mathrm{pit(0T)}}$ reduce from 0.038 to 0.018 V. It indicates that the inhibition of pitting susceptibility and corrosion rate by magnetic field decrease with increasing concentration of NaCl solution

The corrosion process of metals is related to oxidation (anodic reaction) and oxidant reduction (cathodic reaction). When the magnetic field is applied, the mass transfer is influenced by the magnetohydrodynamic (MHD) flow on Al-solution interface, and the activation/dissolution of the Al anode in NaCl solution is changed. This explains the effect of the electrode preparation process by applying a magnetic field to the Al-3.0Mg mixture. In the electrochemical system, the MHD flow can be calculated using the following equation: $\vec{F}_{\mathrm{MHD}}=\vec{J}\times\vec{B}$, where $\vec{J}$ is the local ion flux.

In an electrochemical system, the orientation of the electronic field can usually determine the ion flux orientation. Therefore, in the corrosion process, the mass transfer rate is significantly affected by the direction of the magnetic field. When the direction of the magnetic field is perpendicular to the electronic field and ion flux, $\vec{F}_{\mathrm{MHD}}$ has the largest value. In addition, the magnetic field induces an additional Lorentz force, which leads the charged particles to penetrate the interfacial diffusion layer.

Aluminum anodic dissolution contains two reactions[31,32]. First, the intermediate ions, *i e*, $\mathrm{Al}^{+}_{(\mathrm{ad})}$ are formed from aluminum after losing electrons. Then, the Al^{3+} ions can be produced from intermediate $\mathrm{Al}^{+}_{(\mathrm{ad})}$ ions through the additional loss of electrons. Both the Al^{3+} ions and the intermediate $\mathrm{Al}^{+}_{(\mathrm{ad})}$ ions have a reaction with O_2, H_2O, and Cl^-, the anode is decomposed, and the passivation film is destroyed. The electrons can freely move and the ions recombine, which contributes to the corrosion of Al-3.0Mg alloy. To our opinion, the depletion of Al^{3+} is the main factor that maintains the corruption progress.

$$\mathrm{Al}-e\rightarrow\mathrm{Al}^{+}_{(\mathrm{ad})} \tag{1}$$

$$\mathrm{Al}^{+}_{(\mathrm{ad})}-2e\rightarrow\mathrm{Al}^{3+} \tag{2}$$

The application of the magnetic field can influ-

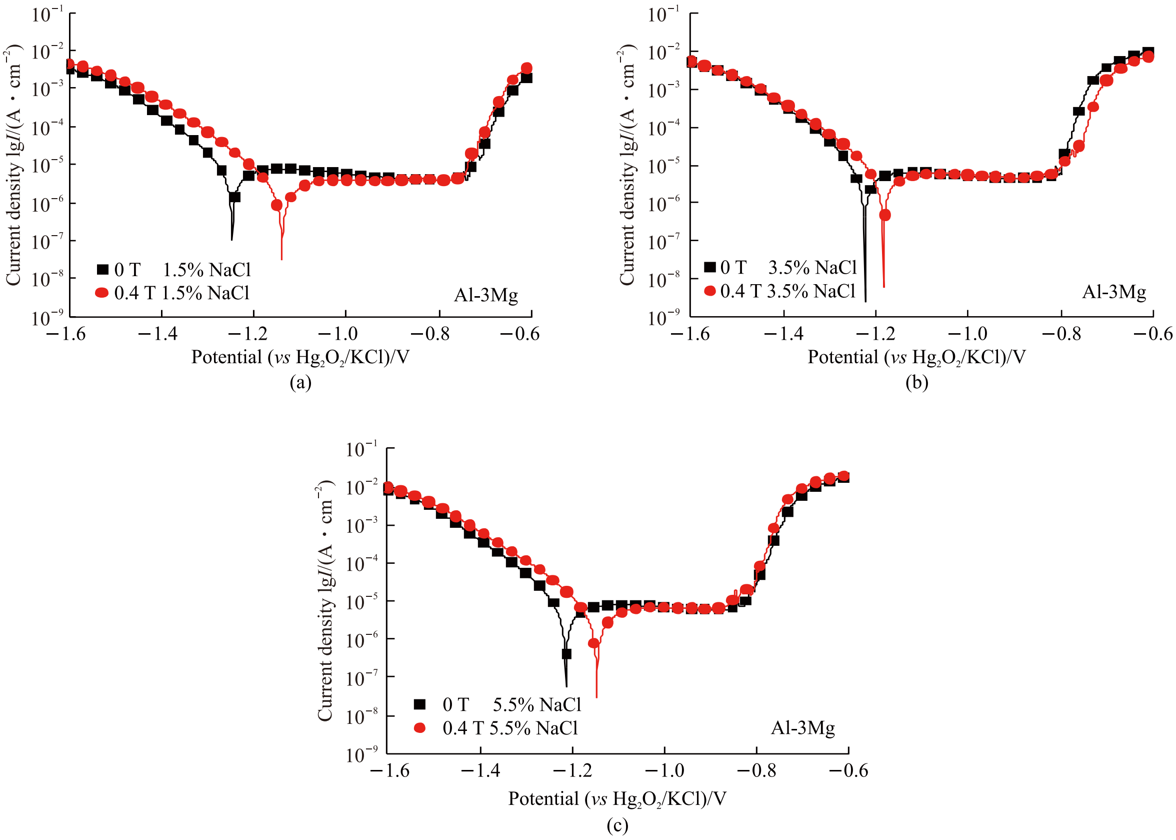

(a)

(b)

(c)

Fig.6 Potentiodynamic polarization curves of Al-3.0Mg alloy in NaCl solution in the absence of magnetic field and under a magnetic field with the strength of 0.4 T: (a) 1.5wt% NaCl; (b) 3.5wt% NaCl; (c) 5.5wt% NaCl

Table 3 **Values of E_{corr}, i_{corr}, and E_{pit} obtained from the polarization curves of Al-3.0Mg alloy tested in 1.5wt%/3.5wt%/5.5wt% NaCl solution in the absence of a magnetic field and under a magnetic field with the strength of 0.4 T**

		E_{corr}/ V		$E_{corr(0.4T)}-E_{corr(0T)}$ /V	i_{corr}/(μA·cm^{-2})		$i_{corr(0.4T)}-i_{corr(0T)}$ /(μA·cm^{-2})	E_{pit}/V		$E_{pit(0.4T)}-E_{pit(0T)}$ /V
		0 T	0.4 T		0 T	0.4 T		0 T	0.4 T	
Al-3.0Mg	1.5%	−1.248	−1.144	0.144	4.474	3.124	−1.350	−0.777	−0.739	0.038
	3.5%	−1.216	−1.186	0.030	7.253	6.670	−0.583	−0.821	−0.799	0.022
	5.5%	−1.211	−0.143	0.068	8.263	7.953	−0.310	−0.837	−0.819	0.018

ence the motion of cations and anions through "paramagnetic gradient force"[33,34]. Due to the presence of magnetic field, the paramagnetic ions are subject to another driving force, which leads to the gradient in the concentration of the paramagnetic ions with the same direction as the gradient of paramagnetic ions. This driving force resulted in the redistribution of the paramagnetic ions in the diffusion layer, causing the paramagnetic ions more concentrated.

$Al^{+}_{(ad)}$ ion has the electron configuration of $1S^22S^22P^63S^13P^1$. The orbits of 3S and 3P only have a single electron, which indicates the paramagnetism of $Al^{+}_{(ad)}$ ions. Therefore, in the presence of a magnetic field, $Al^{+}_{(ad)}$ ions are accumulated around the aluminum electrode. When Al-3.0Mg alloy is corroded in NaCl solution, the paramagnetic gradient force moves the produced $Al^{+}_{(ad)}$ ions closer to the aluminum electrode, leading to a larger amount of $Al^{+}_{(ad)}$ ions on top of the electrode. As a result, the reaction (1) is slowed down and the number of the generated Al^{3+} ions become smaller. Therefore, the application of a magnetic field reduces the concentration of the ions in the diffusion layer, thereby reducing the corrosion sensibility and the corrosion rate of Al-3.0Mg alloy.

With the increase of NaCl concentration, the amount of chloride ions increases, which can increase the corrosion rate of Al-3.0Mg alloys. Under the action of Lorentz force, the chloride ions move faster, which is conducive to destroying the passivation film on of Al-3.0Mg alloy, increasing corrosion rate. Therefore, the higher concentration of NaCl solution, the greater the acceleration effect of magnetic field on corrosion rate and pitting generation of Al-3.0Mg alloys. Under the combined influence of paramagnetic gradient force (Corrosion inhibition) and Lorentz force (Corrosion promotion), the increase in NaCl concentration reduced the inhibition of pitting sensitivity and corrosion rate of Al-3.0Mg alloys by magnetic field.

Fig.7 illustrates the corroded surface of Al-3.0Mg-0.2R_E alloy after immersion in NaCl solutions with concentrations of 1.5wt%, 3.5wt%, and 5.5wt% in the absence and presence of a magnetic field of 0.4 T. With the application of a 0.4 T magnetic field, the pitting holes of Al-3.0Mg-0.2R_E alloys in all NaCl solutions are smaller and fewer than those in the absence of a magnetic field. However, when the concentration of NaCl solution is high, the difference in the amount and dimension of pitting holes between the results with and in the absence of magnetic field become smaller. This indicates that magnetic field can inhibit the generation and growth of pitting holes on the Al-3.0Mg-0.2R_E alloy. But the inhibiting effect is weakened with the increase of NaCl concentration.

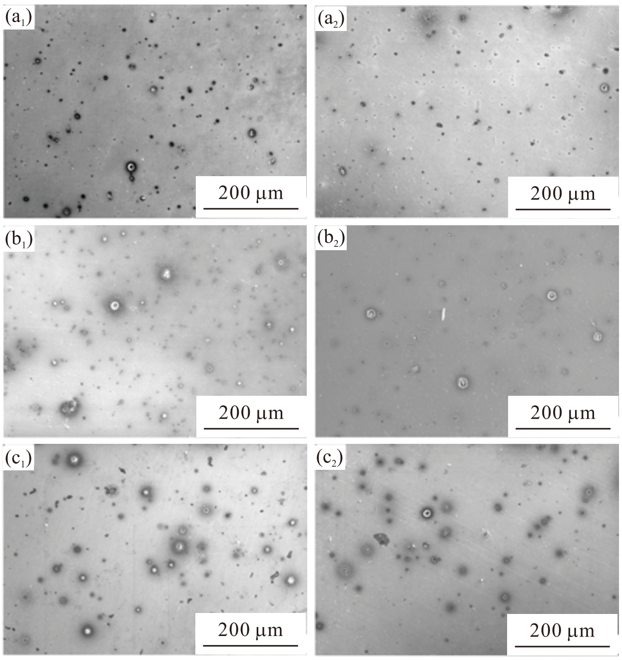

Fig.7 Surface morphologies of corroded Al-3.0Mg-0.2R_E alloy in NaCl solution in the absence of magnetic field and under a magnetic field with the strength of 0.4 T: (a_1) 1.5% NaCl, 0 T; (a_2) 1.5% NaCl, 0.4 T; (b_1) 3.5% NaCl, 0 T; (b_2) 3.5% NaCl, 0.4 T; (c_1) 5.5% NaCl, 0 T; (c_2) 5.5% NaCl, 0.4 T

Fig.8 illustrates the corroded surface of Al-3.0Mg-1.0R_E alloys after immersion in NaCl solutions with concentrations of 1.5wt%, 3.5wt%, and 5.5wt% in the absence of a magnetic field and with a 0.4 T magnetic field. When Al-3.0Mg-1.0R_E samples were immersed in NaCl solutions with the concentrations of 1.5wt% and 3.5wt% under a magnetic field of 0.4 T, fewer and smaller pitting holes were generated than in the absence of a magnetic field. However, when Al-3.0Mg-1.0R_E samples were immersed in NaCl solution with the concentration of 5.5wt% under a magnetic field with the strength of 0.4 T, more and bigger pitting holes were produced than in the absence of magnetic field. The result indicates that magnetic field have an inhibiting effect on the generation and growth of pitting holes of Al-3.0Mg-1.0R$_E$ alloy in low concentration NaCl solution (1.5wt% and 3.5wt%), and have a promoting effect on the production and development of pitting holes in high concentration NaCl solution (5.5wt%).

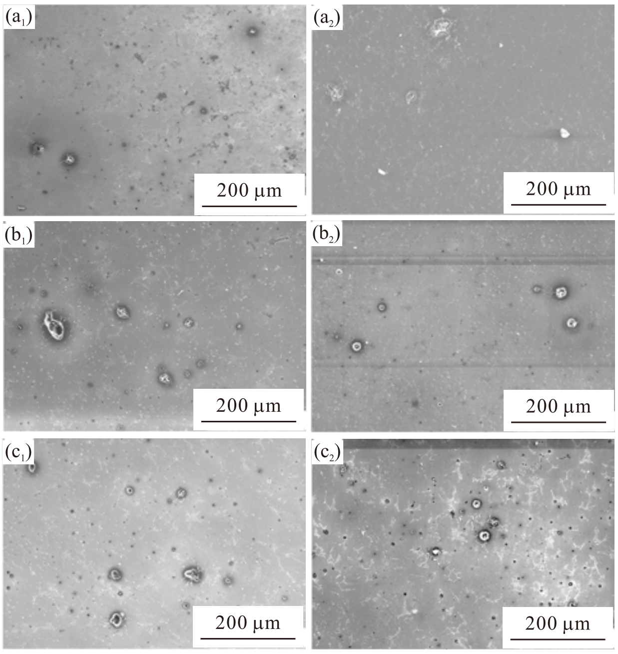

Fig.8 Surface morphologies of corroded Al-3.0Mg-1.0R$_E$ alloy in NaCl solution in the absence of magnetic field and under a magnetic field with the strength of 0.4 T: (a$_1$) 1.5% NaCl, 0 T; (a$_2$) 1.5% NaCl; 0.4 T; (b$_1$) 3.5% NaCl, 0 T; (b$_2$) 3.5% NaCl, 0.4 T; (c$_1$) 5.5% NaCl, 0 T; (c$_2$) 5.5% NaCl, 0.4 T

Fig.9 illustrates the potentiodynamic polarization curves of Al-3.0Mg-xR$_E$ alloy in the absence of a magnetic field and under a magnetic field with the strength of 0.4 T. The values of E_{corr}, i_{corr}, and E_{pit} of the alloys are listed in Table 4. In the presence of a magnetic field, E_{corr} of Al-3.0Mg-xR$_E$ alloys in NaCl solutions with the concentrations of 1.5wt%, 3.5wt%, and 5.5wt% shift positively. In the presence of a magnetic field, the uniform corrosion sensitivity of Al-3.0Mg-xR$_E$ alloys decreases.

For Al-3.0Mg-0.2R$_E$ alloys, under a magnetic field with the strength of 0.4 T, the values of i_{corr} in NaCl solutions are smaller than those in the absence of magnetic field, while the values of E_{pit} are larger than those in the absence of magnetic field. In the presence of a magnetic field, the pitting sensitivity and corrosion rate of Al-3.0Mg-0.2R$_E$ alloy are reduced. However, with the increase of NaCl concentration, $i_{\text{corr(0.4T)}}-i_{\text{corr(0T)}}$ values increase from -1.033 to -0.968 μA·cm^{-2}, while $E_{\text{pit(0.4T)}}-E_{\text{pit(0T)}}$ values drop from 0.023 to 0.016 V. This result indicates that at a higher concentration of NaCl solution, the magnetic field have a weaker inhibiting effect on the pitting sensitivity and corrosion rate.

The impact of the presence of magnetic field on the corrosion behavior of Al-3.0Mg-1.0R$_E$ alloy in NaCl solutions changes with the solution concentrations. In NaCl solutions with concentrations of 1.5wt% and 3.5wt%, the presence of magnetic field can reduce i_{corr}, increase E_{pit}, and lower down the pitting sensitivity and corrosion rate of the alloys. As NaCl concentration become higher, the difference between $i_{\text{corr(0.4T)}}$ and $i_{\text{corr(0T)}}$, $E_{\text{pit(0.4T)}}$, and $E_{\text{pit(0T)}}$ both become smaller. Thus, the magnetic field have a weaker inhibiting effect on pitting sensitivity and corrosion rate. In 5.5wt% NaCl solution, under 0.4 T magnetic field, i_{corr} value is higher and E_{pit} value is smaller than that in the absence of magnetic field. Therefore, in NaCl solution with the concentration of 5.5wt%, in the presence of magnetic field, the pitting sensitivity and corrosion rate of Al-3.0Mg-1.0R$_E$ alloys increase.

As stated above, when rare-earth was added into the alloys, there were fewer skeletal FeAl$_3$ phases (cathode phase) and more skeletal Al$_4$Ce/Al$_4$La phases (anode). Al$_4$Ce/Al$_4$La acts as the anode phases and caused themselves to corrode. As a result, the passivation films forming on the alloys are damaged. The application of a magnetic field cause Ce^{3+} and La^{3+} to move faster from the alloys to the alloy/solution interface and react with oxygen. As the concentration of sodium chloride increases, more chloride ions are involved in the destruction of the passivation film. The magnetic field can accelerate the moving of chloride ions toward the passivation films. As a result, the more Al$_4$Ce/Al$_4$La phases and more chloride ions present in the corrosion process, the more serious passivation films are destroyed. Therefore, in NaCl solution with the concentration of 5.5wt%, when 0.4 T magnetic field is applied, the corrosion rate of Al-3.0Mg-1.0R$_E$ alloy is faster.

Fig.10 shows the corroded surface of Al-3.0Mg-0.2Fe alloys after immersion in NaCl solutions with concentrations of 1.5wt%, 3.5wt%, and 5.5wt% in the presence of a magnetic field and under a magnetic field with the strength of 0.4 T. Under a magnetic field with the strength of 0.4 T, smaller and fewer pitting holes are generated on Al-3.0Mg-0.2Fe alloys in NaCl solutions than those in the absence magnetic field. Similar to Al-3.0Mg-0.2R$_E$ alloy, the difference in the amount and dimension of pitting holes on Al-3.0Mg-0.2Fe alloys between the results in the absence of magnetic field and under a magnetic field with the strength of 0.4 T become smaller in the NaCl solutions with higher concentrations. The result indicates that at a higher NaCl concentration, magnetic field have a weaker inhibiting effect on the corrosion of Al-3.0Mg-0.2R$_E$ alloys.

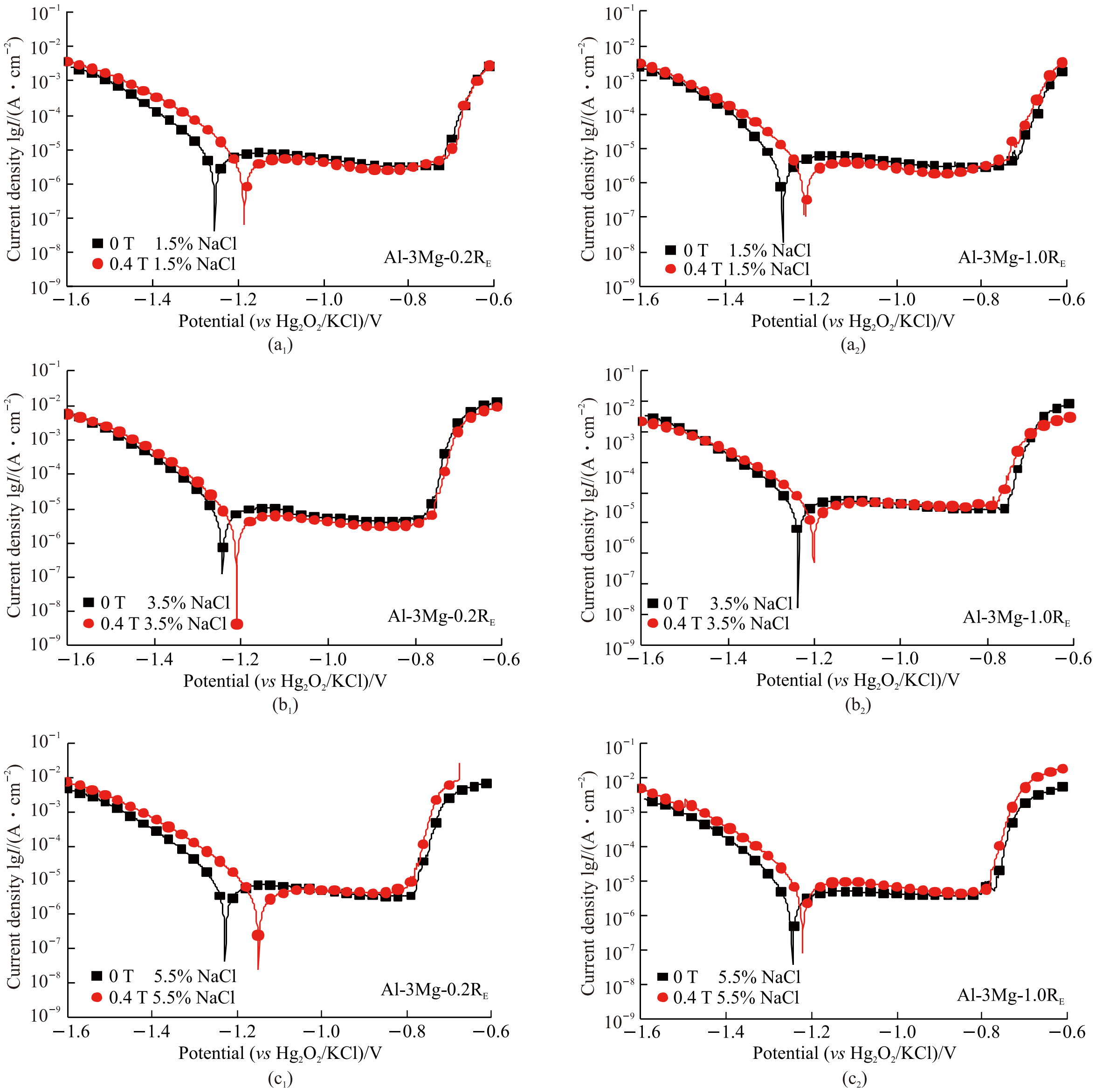

(a_1) (a_2)

(b_1) (b_2)

(c_1) (c_2)

Fig.9 Potentiodynamic polarization curves of Al-3.0 Mg-0.2R$_E$ alloy (1) and Al-3.0 Mg-1.0R$_E$ alloy (2) in NaCl solution in the absence of magnetic field and under a magnetic field with the strength of 0.4 T: (a) 1.5wt% NaCl; (b) 3.5wt% NaCl; (c) 5.5wt% NaCl

Table 4 Values of E_{corr}, i_{corr}, and E_{pit} from the polarization curves of Al-3.0Mg-xR$_E$ alloys tested in 1.5wt%/3.5wt%/5.5wt% NaCl solution in the absence of a magnetic field and under a magnetic field with the strength of 0.4 T

		E_{corr}/ V		$E_{corr(0.4T)}-E_{corr(0T)}$ /V	i_{corr}/(μA·cm^{-2})		$i_{corr(0.4T)}-i_{corr(0T)}$ /(μA·cm^{-2})	E_{pit}/V		$E_{pit(0.4T)}-E_{pit(0T)}$ /V
		0 T	0.4 T		0 T	0.4 T		0 T	0.4 T	
Al-3.0Mg-0.2R$_E$	1.5%	−1.256	−1.189	0.067	3.566	2.533	−1.033	−0.740	−0.717	0.023
	3.5%	−1.243	−1.193	0.050	6.788	5.815	−0.973	−0.793	−0.773	0.020
	5.5%	−1.232	−1.149	0.083	8.518	7.650	−0.868	−0.808	−0.792	0.016
Al-3.0Mg-1.0R$_E$	1.5%	−1.269	−1.216	0.053	4.721	3.813	−0.908	−0.765	−0.741	0.024
	3.5%	−1.261	−1.218	0.043	9.130	8.759	−0.371	−0.836	−0.819	0.017
	5.5%	−1.248	−1.124	0.124	9.873	11.111	1.238	−0.841	−0.851	−0.010

Fig.11 illustrates the corroded surface of Al-3.0Mg-1.0R$_E$ alloys after immersion in NaCl solutions with concentrations of 1.5wt%, 3.5wt%, and 5.5wt% in the absence of a magnetic field and under a magnetic field of the strength of 0.4 T. Under a magnetic field with the strength of 0.4 T, fewer pitting holes are produced on the surface of Al-3.0Mg-1.0Fe alloys in NaCl solutions than those in the absence of a magnetic field. In the NaCl solution with a higher concentration, the difference of pitting holes amount between

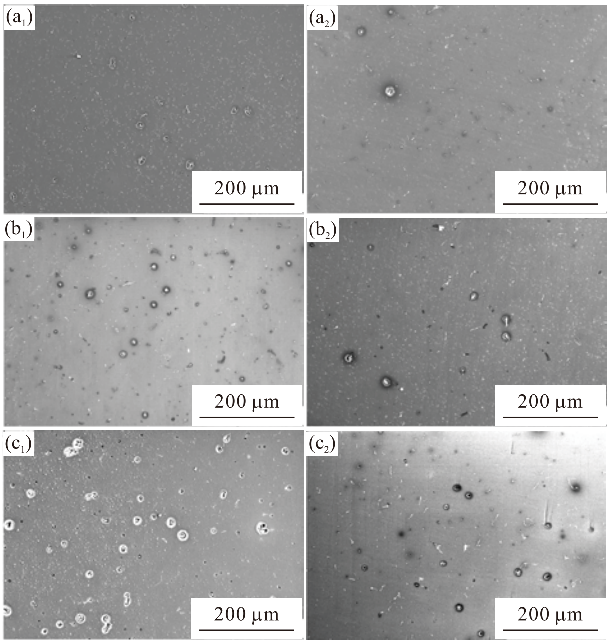

Fig.10 Surface morphologies of corroded Al-3.0Mg-0.2Fe alloy in NaCl solution in the absence of magnetic field and under a magnetic field with the strength of 0.4 T: (a_1) 1.5% NaCl, 0 T; (a_2) 1.5% NaCl, 0.4 T; (b_1) 3.5% NaCl, 0 T; (b_2) 3.5% NaCl, 0.4 T; (c_1) 5.5% NaCl, 0 T; (c_2) 5.5% NaCl, 0.4 T

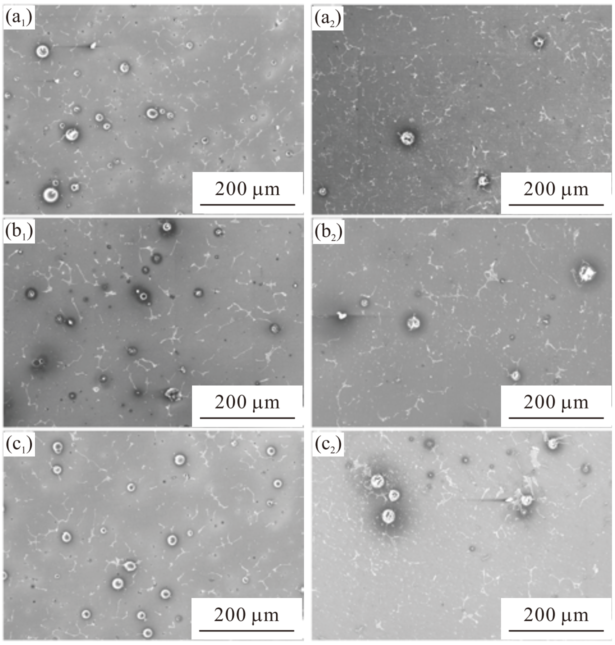

Fig.11 Surface morphologies of corroded Al-3.0Mg-1.0Fe alloy in NaCl solution in the absence of magnetic field and under a magnetic field with the strength of 0.4 T: (a_1) 1.5% NaCl, 0 T; (a_2) 1.5% NaCl, 0.4 T; (b_1) 3.5% NaCl, 0 T; (b_2) 3.5% NaCl, 0.4 T; (c_1) 5.5% NaCl, 0 T; (c_2) 5.5% NaCl, 0.4 T

the results in the absence of magnetic field and under a magnetic field with the strength of 0.4 T become smaller. The magnetic field can inhibit the generation of pitting corrosion of Al-3.0Mg-1.0Fe alloy. But the inhibiting effect is weaker at a higher concentration of NaCl solution. In NaCl solutions with the concentrations of 1.5wt% and 3.5wt%, the presence of a 0.4 T magnetic field led to a smaller dimension of the pitting holes. However, in 5.5wt% NaCl solution, the presence of a 0.4 T magnetic field led to a bigger dimension of pitting holes on Al-3.0Mg-1.0Fe alloy. The results indicates that magnetic field have an inhibiting effect on the growth of pitting holes on the surface of Al-3.0Mg-1.0Fe alloy in low-concentration NaCl solution (1.5wt% and 3.5wt%) and a promoting effect on the growth of pitting holes in high-concentration NaCl solution (5.5wt%).

Fig.12 plots the potentiodynamic polarization curves of Al-3.0Mg-xFe alloys in the absence of a magnetic field and under a magnetic field with the strength of 0.4 T. The values of E_{corr}, i_{corr}, and E_{pit} of the alloys are listed in Table 5. In NaCl solution with concentrations of 1.5wt%, 3.5wt%, and 5.5wt%, in the presence of magnetic field, E_{corr} and E_{pit} of Al-3.0Mg-*x*Fe alloys shift positively. Thus, in the presence of magnetic field, the uniform and pitting sensitivity of Al-3.0Mg-*x*Fe alloys is reduced. At a higher NaCl concentration, the values of $E_{pit(0.4T)}-E_{pit(0T)}$ of Al-3.0Mg-*x*Fe alloys decreased, which indicates that at a higher concentration of NaCl solution, the presence of a magnetic field have a weaker inhibiting effect on the pitting sensitivity.

In the presence of a magnetic field, the values of i_{corr} of Al-3.0Mg-0.2Fe alloys are decreased. The application of a magnetic field cause the corrosion rate of Al-3.0Mg-0.2Fe alloy to decrease. However, with the increase of NaCl concentration, the values of $i_{corr(0.4T)}-$

Table 5 Values of E_{corr}, i_{corr}, and E_{pit} from the polarization curves of Al-3.0Mg-*x*Fe alloys tested in 1.5wt%/3.5wt%/5.5wt% NaCl solution in the absence of a magnetic field and under a magnetic field with the strength of 0.4 T

		E_{corr}/ V		$E_{corr(0.4T)}-E_{corr(0T)}$ /V	$i_{corr}/(\mu A\cdot cm^{-2})$		$i_{corr(0.4T)}-i_{corr(0T)}$ $/(\mu A\cdot cm^{-2})$	E_{pit}/V		$E_{pit(0.4T)}-E_{pit(0T)}$ /V
		0 T	0.4 T		0 T	0.4 T		0 T	0.4 T	
Al-3.0Mg-0.2Fe	1.5%	−1.261	−1.157	0.104	6.070	3.690	−2.380	−0.773	−0.740	0.033
	3.5%	−1.240	1.214	0.026	10.301	8.586	−1.715	−0.841	−0.819	0.022
	5.5%	−1.173	−1.139	0.034	10.991	9.724	−1.267	−0.851	−0.832	0.019
Al-3.0Mg-1.0Fe	1.5%	−1.099	−1.040	0.059	7.331	5.439	−1.892	−0.749	−0.715	0.034
	3.5%	−1.073	−1.017	0.056	8.408	7.170	−1.238	−0.805	−0.783	0.022
	5.5%	−1.053	−1.021	0.032	11.661	12.667	1.006	−0.811	−0.805	0.006

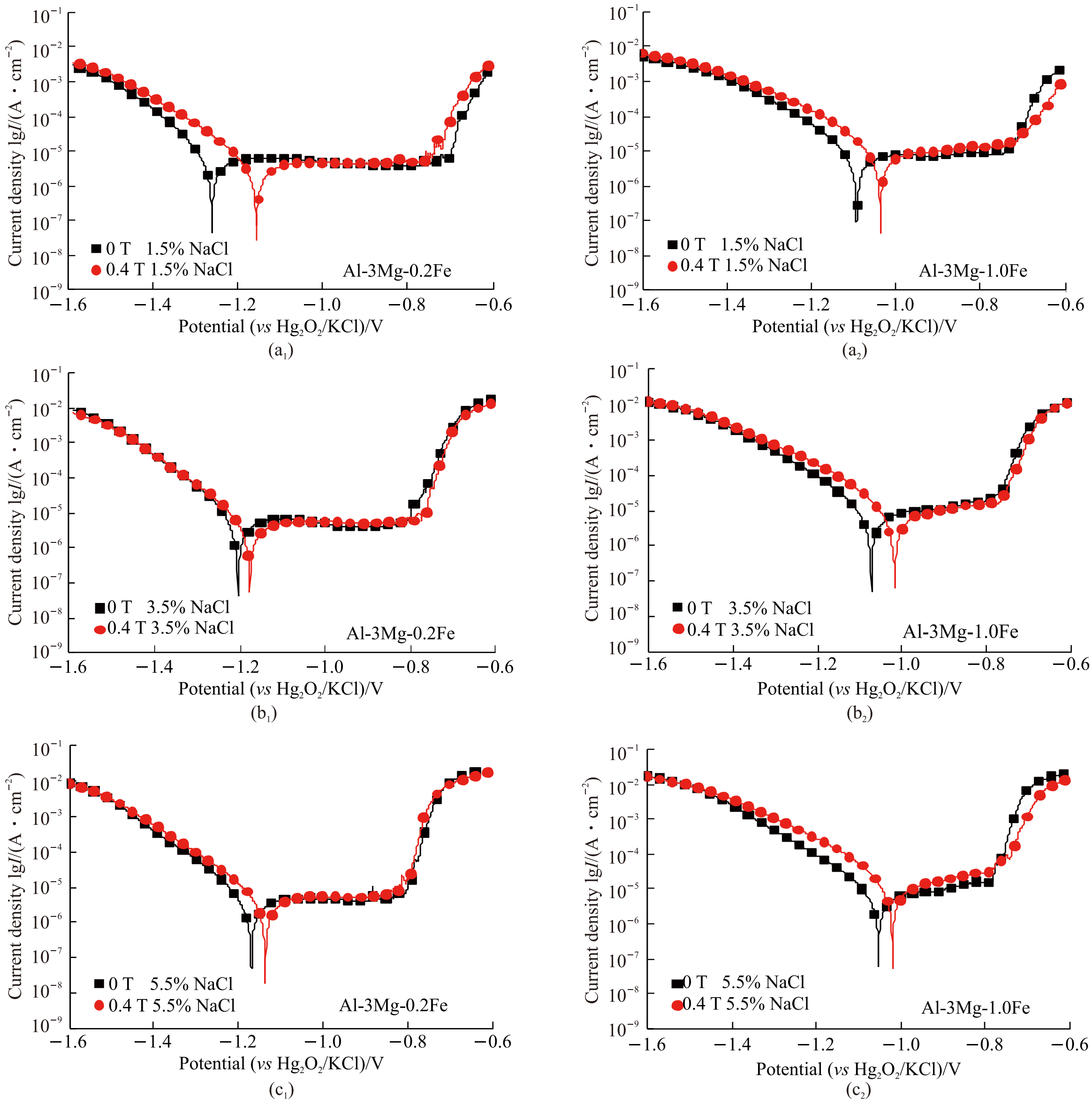

(a_1) (a_2)

(b_1) (b_2)

(c_1) (c_2)

Fig.12 Potentiodynamic polarization curves of Al-3.0 Mg-0.2Fe alloy (1) and Al-3.0 Mg-1.0Fe alloy (2) in NaCl solution in the absence of magnetic field and under a magnetic field with the strength of 0.4 T: (a) 1.5wt% NaCl; (b) 3.5wt% NaCl; (c) 5.5wt% NaCl

$i_{corr(0T)}$ increase from −2.380 to −1.267 μA·cm^{-2}. At a higher concentration of NaCl solution, magnetic field have a weaker inhibiting effect on the corrosion rate of Al-3.0Mg-0.2Fe alloy.

The impact of magnetic field on the corrosion rate of Al-3.0Mg-1.0Fe alloys vary as the concentration of NaCl solution change. In NaCl solutions with the concentrations of 1.5wt% and 3.5wt%, the presence of magnetic field can reduce i_{corr} and corrosion rate of the alloys. As NaCl concentration increase, the difference between $i_{corr(0.4T)}$ and $i_{corr(0T)}$ become smaller. The inhibiting effect of magnetic field on corrosion rate decrease. In the NaCl solutions with the concentration of 5.5wt%, applying a magnetic field of 0.4 T can increase the i_{corr} values. Therefore, the presence of a magnetic field increase the corrosion rate of Al-3.0Mg-1.0R$_E$ alloys in 5.5wt% NaCl solution.

The addition of Fe into the alloys results in an obvious increase in the amount and dimension of skeletal $FeAl_3$ phases (cathode phase). $FeAl_3$ phases act as cathode phases, speed up the corrosion of aluminum matrix corrode themselves, and cause the destruction of the passivation films on the surface of alloys. Therefore, more areas of pitting corrosion appear.

With the increase of NaCl concentration, more chloride ions move to the areas with more pitting corrosion. With the presence of a magnetic field, the movement of chloride ions is accelerated, and the damage rate by chloride ions become fast. As a result, in high-concentration NaCl solution, applying a magnetic field of 0.4 T cause the Al-3.0Mg-1.0Fe alloy to corrode faster.

4 Conclusions

a) As the NaCl concentration increased, the values of E_{corr} and i_{corr} of Al-3.0Mg-xR$_E$/Fe alloys increased, while the value of E_{pit} decreased. When Al-3.0Mg-xR$_E$/Fe alloys were immersed in the higher concentration NaCl solution, more and bigger pitting holes were produced on the surface of the alloys. The corrosion rate and pitting corrosion potential of Al-3.0Mg-xR$_E$/Fe alloys were higher in the higher concentration of NaCl solution.

b) In the presence of magnetic fields, the pitting sensitivity and corrosion rate of Al-3.0Mg, Al-3.0Mg-0.2R$_E$, and Al-3.0Mg-0.2Fe alloys in NaCl solutions with concentrations of 1.5wt%, 3.5wt%, and 5.5wt% were lower. However, with the increase of NaCl concentration, the inhibiting effect of the magnetic field on pitting sensitivity and corrosion decreased.

c) The application of a magnetic field could lower down the pitting sensitivity and corrosion rate of Al-3.0Mg-1.0R$_E$ and Al-3.0Mg-1.0Fe alloys in NaCl solutions with the concentrations of 1.5wt% and 3.5wt%. However, the magnetic field could increase the corrosion rate of the alloys in the NaCl solution with the concentration of 5.5wt%.

References

[1] Cho CH, Son HW, Lee JC, *et al*. Effect of High Mg Content and Processing Parameters on Portevin-Le Chatelier and Negative Strain Rate Sensitivity Effects in Al-Mg Alloys[J]. *Mater. Sci. Eng.*, 2020, 779: 139 151

[2] Saravanan S, Raghukandan K. Microstructure and Mechanical Strength Predicative Modeling in Al 5052-Trapezoidal Grooved SS 304 Explosive Cladding[J]. *J. Wuhan Univ. Technol.*, 2020, 35(5): 958-966

[3] Gao TJ, Yao YJ, Wang XK, *et al*. Effect of Interface Friction on Overlapping Sheets Bulging Formability and Microstructure of 5A02 Aluminum Alloy[J]. *J. Wuhan Univ. Technol.*, 2019, 34(4): 919-924

[4] Beura VK, Kale C, Srinivasan S, *et al*. Corrosion Behavior of a Dynamically Deformed Al-Mg Alloy[J]. *Electrochim. Acta*, 2020, 384: 136 695

[5] Zhang H, Gu DD, Dai DH, *et al*. Influence of Heat Treatment on Corrosion Behavior of Rare Earth Element Sc Modified Al-Mg Alloy Processed by Selective Laser Melting[J]. *Appl. Surf. Sci.*, 2020, 509: 145 330

[6] Fan LT, Ma JJ, Zou CX, *et al*. Reveling Foundations of the Intergranular Corrosion of 5xxx and 6xxx Al Alloys[J]. *Mater. Lett.*, 2020, 271: 127 767

[7] Zhang Q, Zhang PL, Yu ZS, *et al*. Microstructure and Properties of an Al 6061/Galvanized Plate Fabricated by CMT Welding[J]. *J. Wuhan Univ. Technol.*, 2020, 35(5): 937-945

[8] Qi X, Sun B, Chen XM, *et al*. Localized Corrosion and Stress Corrosion Cracking Behavior of AA7003 in a 3.5wt% NaCl Aqueous Solution[J]. *J. Wuhan Univ. Technol.*, 2020, 35(5): 986-995

[9] Jiang G, Bai ZH, Luo BH, *et al*. Effects of Different Electrolytes on Stress Corrosion Properties of 2A12 Aluminum Alloy[J]. *J. Wuhan Univ. Technol.*, 2021, 36(3): 400-406

[10] Cui TF, Liu DX, Shi PA, *et al*. Effect of Stress and Galvanic Factors on the Corrosion Behave of Aluminum Alloy[J]. *J. Wuhan Univ. Technol.*, 2018, 33(3): 688-696

[11] Hinds G, Coey JMD, Lyons MEG. Influence of Magnetic Forces on Electrochemical Mass Transport[J]. *Electrochem. Commun.*, 2001, 3: 215-218

[12] Aaboubi O, Chopart JP, Douglade J, *et al*. Magnetic Field Effects on Mass Transport[J]. *J. Electrochem. Soc.*, 1990, 137: 1 796-1 804

[13] Zhang P, Zhu Q, Su Q, *et al*. Corrosion Behavior of T2 Copper in 3.5% Sodium Chloride Solution Treated by Rotating Electromagnetic Field[J]. *Trans. Nonferrous Metals Soc. China*, 2016, 26: 1 439-1 446

[14] Hu J, Dong CF, Li XG, *et al*. Effects of Applied Magnetic Field on Corrosion of Beryllium Copper in NaCl Solution[J]. *J. Mater. Sci. Technol.*, 2010, 26: 355-361

[15] Chiba A, Ogawa T. Effects of Magnetic Field Direction on the Dissolution of Copper, Zinc, and Brass in Nitric Acid[J]. *Corros. Eng.*, 1989, 38: 523-528

[16] Devos O, Aaboubi O, Chopart JP, *et al*. EIS Investigation of Zinc Electrodeposition in Basic Media at Low Mass Transfer Rates Induced by a Magnetic Field[J]. *J. Phys. Chem. B*, 1999, 103: 496-501

[17] Sueptitz R, Koza J, Uhlemann M, *et al*. Magnetic Field Effect on the Anodic Behavior of a Ferromagnetic Electrode in Acidic Solution[J]. *Electrochim. Acta*, 2009, 54: 2 229-2 233

[18] Espina-Hernandez JH, Caleyo F, Venegas V, *et al*. Pitting Corrosion in Low Carbon Steel Influenced by Remanent Magnetization[J]. *Corrosion Sci.*, 2011, 53: 3 100-3 107

[19] Zhang X, Wang ZH, Zhou ZH, *et al*. Effects of Magnetic Field and Rare Earth Addition on Corrosion Behavior of Al-3.0wt% Mg Alloy[J]. *J. Alloys Compd.*, 2017, 698: 241-249

[20] Zhang X, Wang ZH, Zhou ZH, *et al*. Corrosion Behavior of Al-3.0 wt.%Mg Alloy in NaCl Solution under Magnetic Field[J]. *Rare Met.*, 2017, 36: 627-634

[21] Zhang X, Wang ZH, Zhou ZH, *et al*. Impact of Magnetic Field on Corrosion Performance of Al-Mg Alloy with Different Electrode Potential Phases[J]. *Intermetallics*, 2021, 129: 107 037

[22] Li XJ, Zhang M, Yuan BY, *et al*. Effect of Magnetic Field on the Corrosion Dissolution of the 304 SSFeCl$_3$ System[J]. *Electrochim. Acta*, 2016, 222: 619-626

[23] Lu Z, Huang C, Huang D, *et al*. Effects of a Magnetic Field on the Anodic Dissolution, Passivation and Transpassivation Behavior of Iron in Weakly Alkaline Solutions with or without Halides[J]. *Corrosion Sci.,* 2006, 48: 3 049-3 077

[24] Lu Z, Yang W. In situ Monitoring the Effects of a Magnetic Field on the Opencircuit Corrosion States of Iron in Acidic and Neutral Solutions[J]. *Corrosion Sci.*, 2008, 50: 510-522

[25] Sueptitz R, Tschulik K, Uhlemann M, *et al*. Impact of Magnetic Field Gradients on the Free Corrosion of Iron[J]. *Electrochim. Acta,* 2010, 55: 5 200-5 203

[26] Eugene J Kelly. Magnetic Field Effects on Electrochemical Reactions Occurring at Metal/Flowing-electrolyte Interfaces[J]. *Electrochim. Soc.*, 1977, 124: 987-994

[27] Despic AR. Electrochemical Properties of Aluminum Alloys Containing Indium, Gallium and Thallium[J]. *J. Appl. Electrochem.*, 1976, 6: 527-542

[28] Zhang X, Wang ZH, Zhou ZH, *et al*. Effects of Cerium and Lanthanum on the Corrosion Behavior of Al-3.0wt%Mg Alloy[J]. *J. Mater. Eng. Perform.*, 2016, 25: 1 122-1 128

[29] Zhang X, Wang ZH, Zhou ZH, *et al*. Influence of Rare Earth (Ce and La) Addition on the Performance of Al-3.0wt%Mg Alloy[J]. *J. Wuhan Univ Technol.*, 2017, 32: 611-618

[30] Huang ZH, Guo XF, Zhang ZM, *et al*. Effects of Ce on Corrosion Resistance of AZ91D Magnesium Alloy[J]. *Acta Metall. Sin.*, 2005, 18: 129-136

[31] Despic AR. Electrochemical Properties of Aluminum Alloys Containing Indium, Gallium and Thallium[J]. *J. Appl. Electrochem.*, 1976, 6: 527-542

[32] Ford FP, Burstein GT, Hoar TP. Bare Surface Reaction Rates and Their Relation to Environment Controlled Cracking of Aluminum Alloys[J]. *J. Electrochem. Soc.*, 1980, 127: 1 325-1 331

[33] O'Brien RN, Santhanam KSV. Electrochemical Hydrodynamics in Magnetic Fields with Laser Interferometry: Influence of Paramagnetic Ions[J]. *J. Appl. Electrochem.*, 1990, 20: 427-437

[34] Waskaas M, Kharkats YI. Effect of Magnetic Fields on Convection in Solutions Containing Paramagnetic Ions[J]. *J. Electron. Chem.*, 2001, 502: 51-57